Application of High-Density Sound Absorbing Materials for Improving Low-Frequency Spectral Flatness in Room Response

Mirosław MEISSNER

Corresponding author: Mirosław MEISSNER, email: mmeissn@ippt.pan.pl

Institute of Fundamental Technological Research, Polish Academy of Sciences, Pawińskiego 5B, 02-106 Warsaw

Abstract A room impulse response obtained for complex-valued boundary conditions on wall surfaces was used to determine the frequency response of arbitrary shaped room. Based on theoretical findings, a numerical procedure was developed to test the effectiveness of a high-density sound absorbing material in improving low-frequency spectral flatness. The impedance of absorbing material was determined using the two-parameter Komatsu model. The simulation results have shown that the smoothing effect of the frequency response becomes apparent when the thickness of absorbing material is large enough. This is because as the material thickness increases, the sound absorption tends to increase at lower frequencies.

Keywords: frequency response of room, spectral flatness, room impulse response, wall impedance

1. Introduction

At low frequencies, the acoustical behavior of enclosures is greatly influenced by excited acoustic modes, resulting in resonant sound fields observed in both frequency, temporal and spatial domains [1–5]. In low-frequency range, the modal density is relatively low, thus, the presence or absence of resonant modes in a specific frequency band leads to uneven frequency responses that are clearly perceived by listeners. This problem is solved applying acoustical treatments which are based a change in a room geometry and a modification of sound absorption distribution on walls. Many studies have investigated the effectiveness of such acoustic treatments through measurements and modeling. The effects of geometric modification of room walls on the frequency response have been investigated by utilizing the finite element analysis [6] and the finite element-based optimization method [7]. To smooth a frequency response in rectangular rooms, attempts have been made to classify room's low frequency sound distribution with regards to its dimension ratios [8, 9]. Special metrics have been proposed for the optimal modal response and from these good dimension ratios have been found [10, 11]. Another technique commonly used for improving room acoustics at low frequencies consists in increasing a sound absorption on room walls. This objective can be achieved by using broadband absorbers [12] or different configurations of sound absorbing materials for acoustic treatment of room [13].

In this paper, the wave-based model is developed to predict the frequency response (FR) of a room. Using the room impulse response determined for complex-valued boundary conditions on room walls, the FR is calculated and this response is used to determine two measures for assessing a spectral flatness of the FR over the low-frequency range. The first measure bases on the level of amplitude spectrum and is defined as the deviation of the FR from a smooth fitted response calculated by the quadratic polynomial regression. The second measure bases on the amplitude spectrum and represents the classical flatness indicator defined as the ratio of the geometric mean of the discrete data to the arithmetic mean. Acoustic properties of high-density sound absorbing materials are determined using the Komatsu model. Changes in the spectral flatness are examined for room walls that are nearly hard acoustically and for the ceiling and lateral walls covered by a rigidly-backed layer of this material of varying thickness. Finally, the simulation data is compared to evaluate the effectiveness of the absorbing material in creating a flatter FR.

2. Theoretical model

In the low-frequency range, the sound pressure p generated inside a room by the volume sound source is a solution of the inhomogeneous wave equation of the form

$$\left[\Delta - \frac{1}{c^2}\frac{\partial^2}{\partial t^2}\right]p(\mathbf{r},t) = -q(\mathbf{r},t), \tag{1}$$

where Δ is the Laplace operator, c is the sound speed, q is the volume source term and $\mathbf{r}=(x,y,z)$ is a position coordinate of a field point. A sound damping in a room system is provided by absorbing material located on room walls. These walls are assumed to be locally reacting to the sound pressure, therefore p must satisfies the following boundary condition on wall surfaces

$$\nabla p \cdot \mathbf{n} = -\frac{1}{\zeta c}\frac{\partial p}{\partial t}, \tag{2}$$

where ∇ is the gradient vector operator, the dot is a scalar product, $\mathbf{n}$ is the outward normal vector and ζ is the normalized wall impedance. The impedance's real part ζ_r represents the normalized resistance, whereas its imaginary part ζ_i is referred to as the normalized reactance. Absorbing properties of room walls are described by the random-incident absorption coefficient α which is related to real and imaginary parts of the wall impedance by the following expression [14]

$$\alpha = \frac{8\zeta_r}{|\zeta|^2}\left[1 - \frac{\zeta_r}{|\zeta|^2}\ln\left(1+2\zeta_r+|\zeta|^2\right) + \frac{\zeta_r^2-\zeta_i^2}{\zeta_i|\zeta|^2}\arctan\left(\frac{\zeta_i}{1+\zeta_r}\right)\right], \tag{3}$$

where $|\zeta|$ is the impedance magnitude. When room dimensions are comparable to the wavelength, the method that is most suitable for solving the wave equation is the modal expansion method. In the modal approach, the room response to a sound excitation is found as a superposition of individual responses of acoustic modes generated inside the room i.e.

$$p(\mathbf{r},t) = \sum_{m=1}^{\infty} p_m(t)\varPhi_m(\mathbf{r}), \tag{4}$$

where p_m are time-dependent modal amplitudes which are complex due to the boundary condition (2), $\varPhi_m$ are the eigenfunctions and $\mathbf{r}=(x,y,z)$ determines the position of a receiving point. For the value of $|\zeta|$ much smaller than unity, the room walls are characterized by a small absorption and in this case it is possible to approximate the functions $\varPhi_m$ by the eigenfunctions determined for hard room walls.

According to the convolution theorem, a general solution of Eq. (1) can be written as [15]

$$p(\mathbf{r},t) = \int_V\int_{-\infty}^{t} q(\mathbf{r}',\tau)h(\mathbf{r}',\mathbf{r},t-\tau)\,d\tau dv', \tag{5}$$

where V is the room volume, h is the room impulse response function, $\mathbf{r}'=(x',y',z')$ determines the position of a source point and $dv'=dx'dy'dz'$. The function h is zero for $t < \tau$ because if an impulse occurs at τ, no effects of the impulse should be present at an earlier time (causality condition). A method for finding the room impulse response was described in Ref. [13] and the obtained result has the following form

$$h(\mathbf{r}',\mathbf{r},t) = c^2\sum_{m=1}^{\infty}\frac{\exp[-(r_m+\mathrm{j}\varphi_m)t]}{\varOmega_m+\mathrm{j}\eta_m}\left[\sin(\varOmega_m t)\cosh(\eta_m t) + \mathrm{j}\cos(\varOmega_m t)\sinh(\eta_m t)\right]\varPhi_m(\mathbf{r}')\varPhi_m(\mathbf{r}), \tag{6}$$

where j is the imaginary unit, the parameters r_m and φ_m in the exponential function are given by

$$r_m = \frac{c}{2}\int_S\frac{\zeta_r\varPhi_m^2(\mathbf{r})}{|\zeta|^2}\,ds, \qquad \varphi_m = -\frac{c}{2}\int_S\frac{\zeta_i\varPhi_m^2(\mathbf{r})}{|\zeta|^2}\,ds, \tag{7a,b}$$

S is the surface area of room walls, the quantities Ω_m and η_m are determined by

$$\Omega_m = \sqrt{\frac{a_m + \sqrt{a_m^2 + b_m^2}}{2}}, \qquad \eta_m = \sqrt{\frac{-a_m + \sqrt{a_m^2 + b_m^2}}{2}}, \tag{8a,b}$$

the parameters a_m and b_m are as follows

$$a_m = \omega_m^2 - r_m^2 + \varphi_m^2, \qquad b_m = -2r_m\varphi_m \tag{9a,b}$$

and ω_m are the natural eigenfrequencies, i.e. the eigenfrequencies for undamped modal vibrations.

The frequency response (FR) of the room is defined as the frequency spectrum of the sound pressure signal $p(\mathbf{r},t)$ received at the observation point $\mathbf{r}$, when the room is excited by a point source with a flat power spectrum. As is well known, the power spectral density is perfectly flat for the impulse excitation, thus the volume source in Eq. (5) is assumed to have the form $q(\mathbf{r}',\tau) = Q\delta(\mathbf{r}'-\mathbf{r}_0)\delta(\tau)$, where $\mathbf{r}_0 = (x_0, y_0, z_0)$ determines a source position and $Q = (8\pi\rho c W)^{1/2}$ [16], where W is the source power and ρ is the air density. From a mathematical point of view, the FR is equivalent to a Fourier transform of $p(\mathbf{r},t)$. Thus, inserting the formula for $q(\mathbf{r}',\tau)$ into Eq. (5) one can obtain

$$P_F(\mathbf{r},\omega) = \int_{-\infty}^{\infty} p(\mathbf{r},t)e^{-j\omega t}dt = Q\int_0^{\infty} h(\mathbf{r}_0,\mathbf{r},t)e^{-j\omega t}dt = Qc^2 \sum_{m=1}^{\infty} \frac{\Phi_m(\mathbf{r}_0)\Phi_m(\mathbf{r})}{\xi_m^2 + \psi_m^2 - \omega^2 + 2j\omega\xi_m}, \tag{10}$$

where ω is the angular source frequency, $\xi_m = r_m + j\varphi_m$ and $\psi_m = \Omega_m + j\eta_m$. Since the pressure P_F is complex, a quantity suitable for predicting the FR is the amplitude spectrum P defined as the magnitude of P_F, i.e.

$$P(\mathbf{r},\omega) = \sqrt{P_F(\mathbf{r},\omega)P_F^*(\mathbf{r},\omega)}, \tag{11}$$

where an asterisk as a superscript denotes the complex conjugate. Thus, after inserting the formula for P_F into Eq. (11) one finds the following expression for the amplitude P

$$P(\mathbf{r},\omega) = \sqrt{\left[\sum_{m=1}^{\infty} A_m \Phi_m(\mathbf{r}_0)\Phi_m(\mathbf{r})\right]^2 + \left[\sum_{m=1}^{\infty} B_m \Phi_m(\mathbf{r}_0)\Phi_m(\mathbf{r})\right]^2}, \tag{12}$$

where the quantities A_m and B_m are given by

$$A_m = \frac{Qc^2\left[r_m^2 + \Omega_m^2 - \eta_m^2 - (\omega + \varphi_m)^2\right]}{\left[(r_m + \eta_m)^2 + (\omega + \varphi_m - \Omega_m)^2\right]\left[(r_m - \eta_m)^2 + (\omega + \varphi_m + \Omega_m)^2\right]}, \tag{13}$$

$$B_m = -\frac{2Qc^2\left[r_m(\omega + \varphi_m) + \Omega_m\eta_m\right]}{\left[(r_m + \eta_m)^2 + (\omega + \varphi_m - \Omega_m)^2\right]\left[(r_m - \eta_m)^2 + (\omega + \varphi_m + \Omega_m)^2\right]}. \tag{14}$$

As is clear from Eqs. (12)–(14), the amplitude spectrum is dependent on the source and receiver positions $\mathbf{r}_0$ and $\mathbf{r}$, and, through the quantities r_m, φ_m, Ω_m, and η_m on the natural eigenfrequency ω_m and the real and imaginary parts of the wall impedance ζ.

3. Numerical study

The presented method for determining the FR applies to enclosures of any shape. However, to perform numerical simulations over a wider frequency band, a rectangular room was chosen because the modal behavior of such a room is well known and described. The assumed dimensions of the room are as follows: $L_x = 10$ m, $L_y = 7$ m, $L_z = 4$ m (Fig. 1). Since they correspond to dimensions of lecture rooms or small music studios, a sound source representing, for example, a speaker or a singer was located at the point: $x_0 = 1.5$ m, $y_0 = 3$ m, $z_0 = 1.6$ m. Since room walls were assumed to provide small sound damping, the eigenfunctions Φ_m were computed from the equation

$$\Phi_m(\mathbf{r}) = \sqrt{\frac{\varepsilon_x \varepsilon_y \varepsilon_z}{V}} \cos\left(\frac{n_x \pi x}{L_x}\right)\cos\left(\frac{n_y \pi y}{L_y}\right)\cos\left(\frac{n_z \pi z}{L_z}\right), \tag{15}$$

where the modal indices n_x, n_y, n_z are non-negative integers which are not simultaneously equal to zero, $\varepsilon_s = 1$ if $n_s = 0$, and $\varepsilon_s = 2$ if $n_s > 0$. The eigenfrequencies ω_m corresponding to these functions are as follows

$$\omega_m = \pi c \sqrt{\left(\frac{n_x}{L_x}\right)^2 + \left(\frac{n_y}{L_y}\right)^2 + \left(\frac{n_z}{L_z}\right)^2}. \tag{16}$$

In numerical simulations, two distributions of sound absorbing materials on room walls were considered. In the first case it was assumed that all room walls are nearly hard acoustically, which means that a magnitude of the wall impedance ζ is large but finite. In numerical model, this requirement was achieved by assuming that $\zeta = 388.75$, which corresponds to the absorption coefficient α of 0.02. In the second case, the floor was still modeled as nearly hard acoustically, while a sound absorbing material was placed on the ceiling and lateral walls to improve a low-frequency spectral flatness.
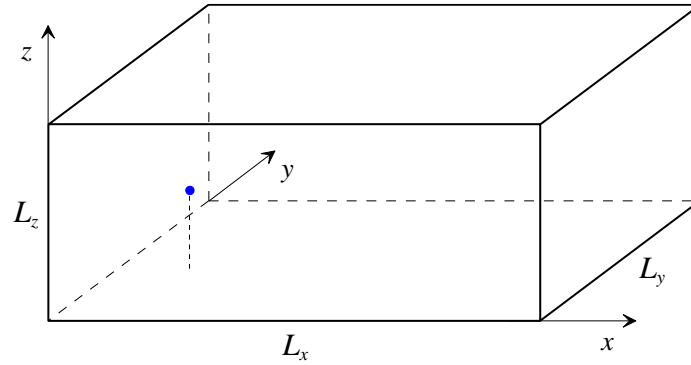

Fig. 1. Rectangular room under study together with the associated coordinate system.
A source position is indicated by a blue point.

The acoustic treatment of a room was carried out using high-density porous sound absorbing material because it exhibit better sound absorption performance at low frequencies as compared to conventional absorbing materials. A rigidly-backed layer of this material was placed on the ceiling and lateral walls and if H is the thickness of this layer, the formula for the wall impedance is expressed as [17]

$$\zeta = -\mathrm{j}\zeta_c \cot(\gamma H), \tag{17}$$

where ζ_c the normalized characteristic impedance of the material and γ is the propagation constant. To predict the acoustic properties of ζ_c and γ, the Komatsu model [18] was used because it is particularly effective for high-density absorbing materials. The Komatsu model is an empirically based two parameter model which specifies ζ_c and γ as a function of the airflow resistivity σ and the sound frequency f

$$\zeta_c = 1 + 0.00027\left(2 - \log\frac{f}{\sigma}\right)^{6.2} - \mathrm{j}0.0047\left(2 - \log\frac{f}{\sigma}\right)^{4.1}, \tag{18}$$

$$\gamma = \frac{2\pi f}{c}\left\{0.0069\left(2 - \log\frac{f}{\sigma}\right)^{4.1} + \mathrm{j}\left[1 + 0.0004\left(2 - \log\frac{f}{\sigma}\right)^{6.2}\right]\right\}. \tag{19}$$

Numerical simulations were performed for the absorbing material with the airflow resistivity σ of 200 kPa·s/m^2 and the layer thickness H of 3 cm, 5 cm and 8 cm. The calculation procedure took into account the change in room dimensions after placing the material on room walls. The FR was predicted in the frequency range 20–1000 Hz at receiving points located at a distance of 1.2 m from the room floor. As the

amplitude spectrum P strongly changes with the frequency, it was decided to present the frequency response using the level L of the amplitude spectrum which is determined by

$$L(\mathbf{r},\omega) = 20\log\left[\frac{P(\mathbf{r},\omega)}{P_{\text{ref}}}\right], \tag{20}$$

where $P_{\text{ref}} = 2\cdot 10^{-5}$ Pa is the reference sound pressure. Exemplary FRs simulated for nearly hard room walls and the absorbing material with the thickness H of 3 cm 8 cm are depicted in Fig. 2. Comparison of these results indicates that the considered frequency range can be divided into two subranges: 20–200 Hz and 200–1000 Hz. In the lower frequency subrange, the FRs for the absorbing material placed on the room ceiling and lateral walls are very different each other because a spectral flatness for the material thickness of 8 cm is much greater than for H of 3 cm. On the other hand, in the frequency subrange 200–1000 Hz the FRs are very similar in both cases and in comparison with the FR for nearly hard room walls, a substantial reduction of the level L is observed. To explain the observed differences in the obtained FRs, the absorption coefficient α was computed for the considered thickness of absorbing material using Eq. (3) and Eqs. (17)–(19). The results are shown in Fig. 3. They prove that for the considered high-density sound absorbing material a frequency dependence of α is very sensitive to the thickness H of the material. An increase in H causes the growth of a sound absorption in the frequency subrange 20–200 Hz, which makes the FR for the highest H much flatter.
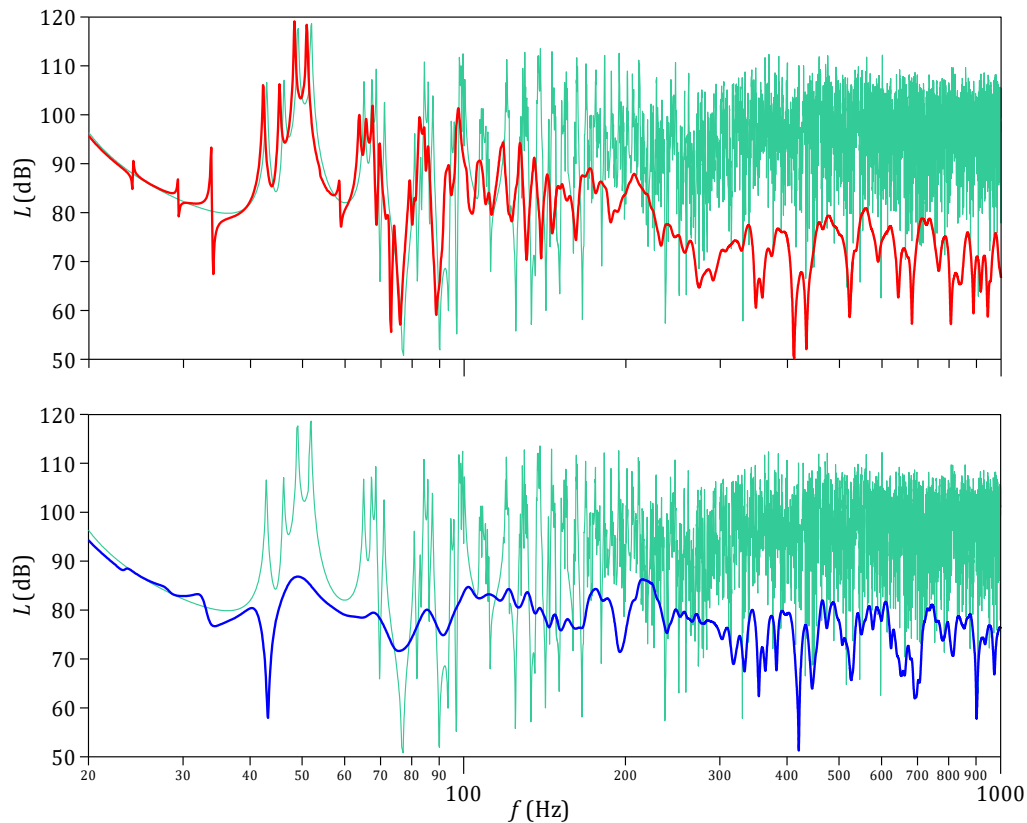

Fig. 2. Comparison of FRs obtained for nearly hard room walls (green lines) and for absorbing material with the thickness of 3 cm (red line) and 8 cm (blue line). The receiver is located at the point: $x = 7.5$ m, $y = 3.5$ m, $z = 1.2$ m.
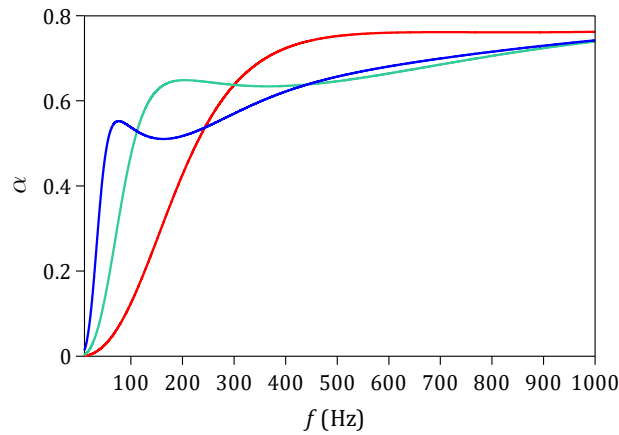
Fig. 3. Frequency-dependence of the absorption coefficient α for assumed thickness of high-density sound absorbing material: 3 cm (red line), 5 cm (green line) and 8 cm (blue line).

To quantify the flatness of the FR, two measures were introduced. The first measure is based on the level L of the amplitude spectrum P and is defined as

$$D(\mathbf{r}) = \sqrt{\frac{1}{N+1} \sum_{n=0}^{N} \left[L(\mathbf{r},\omega_n) - L_c(\mathbf{r},\omega_n) \right]^2}, \tag{21}$$

where $L_c = A\omega^2 + B\omega + C$ is the best-fit curve calculated on the basis of the level L of the amplitude spectrum using the quadratic polynomial regression. The levels L and L_c are determined in the discretized frequency range, i.e. $N = (\omega_u - \omega_l)/\Delta\omega$, $\omega_n = \omega_l + n\Delta\omega$, where ω_l and ω_u are lower and upper limits of the frequency range. The parameter D is expressed in decibels and shows how much the level L deviates from the reference curve L_c which models the flat FR. The second measure represents the classical flatness indicator defined as the ratio of the geometric mean (GM) of the discrete data to the arithmetic mean (AM) [19]. This measure is determined on the basis of discrete set of the amplitude spectrum P, i.e.

$$E(\mathbf{r}) = \frac{\left[\prod_{n=0}^{N} P(\mathbf{r},\omega_n) \right]^{\frac{1}{N+1}}}{\frac{1}{N+1} \sum_{n=0}^{N} P(\mathbf{r},\omega_n)}. \tag{22}$$

Since GM $\le$ AM, the parameter E ranges from zero to one, with the maximum value being reached when the amplitudes $P(\mathbf{r},\omega_n)$ for $n = 0,1,2...N$ are the same. The parameters D and E were computed at receiving points $\mathbf{r}$ which were the nodes of the horizontal mesh with uniform mesh sizes, i.e. $\Delta x = \Delta y = 0.1$ m. The mesh was located at a distance of 1.2 m from the room floor. Calculations were performed in a frequency range with the limits $f_l = 20$ Hz and $f_u = 200$ Hz using the frequency step Δf of 0.1 Hz. The computer program calculates the FR up to the frequency 500 Hz. This additional 300 Hz allows the residues from modes in the region 200–500 Hz to influence the FR below 200 Hz.

Tab. 1. Values of parameters D and E for the FRs shown in Fig. 2.

H (cm)	D (dB)	E
0	11.85	0.433
3	7.76	0.604
8	4.07	0.894

Tab. 2. Minimum, maximum and mean values of the parameters *D* and *E* for nearly hard room walls (*H* equal to zero) and the considered thickness *H* of high-density absorbing material.

H (cm)	D (dB)		E	
	mean	extremes	mean	extremes
0	9.26	6.04–13.78	0.589	0.403–0.781
3	7.23	3.44–10.90	0.654	0.383–0.913
5	5.72	1.91–9.12	0.688	0.326–0.972
8	5.19	1.27–9.85	0.809	0.498–0.986

To find out what values the parameters *D* and *E* take for different FRs, in Tab. 1 calculation results of *D* and *E* for the FRs depicted in Fig. 2 are collected. The case where *H* is equal to zero corresponds to a room where all walls are nearly hard acoustically. Comparing the data in Tab. 1 with graphs in Fig. 2 shows that both parameters respond correctly to changes in the FRs, and therefore they are proper indicators of the spectral flatness. This conclusion is confirmed by the data in Tab. 2 which summarize calculation results obtained at all mesh nodes. Indeed, these data show that the effectiveness of the high-density absorbing material in smoothing the FR increases with increasing the material thickness and that for the greatest *H*, the reduction in *D* of about 4 dB is observed when it comes to mean and maximum value. In the case of the parameter *E*, an increase in the material thickness causes an increase in *E* of about 0.2. The minimum value of *D* and the maximum value of *E* were obtained at the receiving point located just below the source point. As shown in Fig. 4, this is due to the fact that in close proximity to the sound source, the direct sound is dominant due to the small influence of the reflected sound which is the result of highly absorbing room walls.
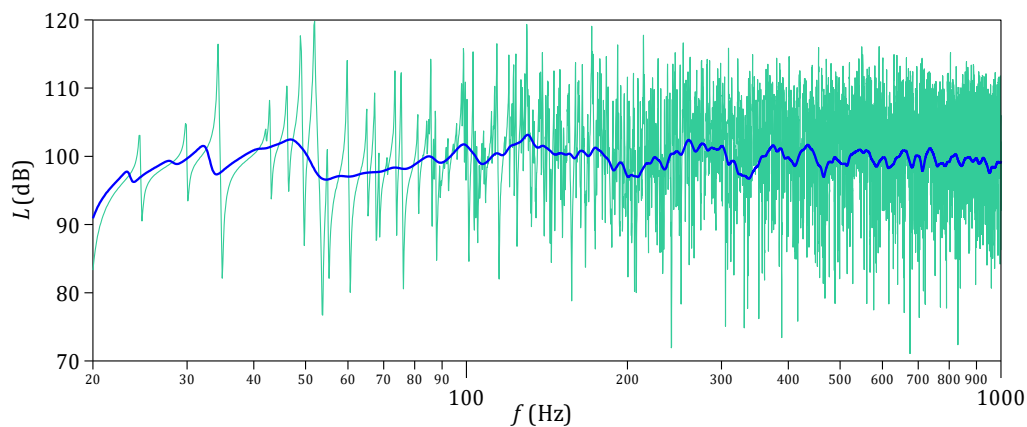

Fig. 4. Comparison of FRs obtained for nearly hard room walls (green line) and for absorbing material with the thickness of 8 cm (blue line). The receiver is located at the point: $x = 1.5$ m, $y = 3$ m, $z = 1.2$ m.

4. Summary and conclusions

In this paper, an application of a high-density sound absorbing material for smoothing the frequency response (FR) of a room was examined. A theoretical model was based on a modal description of the room impulse response which allowed an easy prediction of the FR by applying the inverse Fourier transform. A frequency dependent impedance of the absorbing material was determined using the two-parameter Komatsu model. Theoretical considerations have been accompanied with the numerical study carried out for nearly hard room walls and for acoustic treatment consisting in covering the ceiling and lateral walls with a rigidly-backed layer of absorbing material. The effectiveness of absorbing material in creating a flatter FR was investigated in the frequency range 20–200 Hz using two spectral flatness indicators. Calculation results have shown that an improvement in spectral flatness is significant when a layer

thickness is sufficiently large. This is because as the layer thickness increases, the sound absorption tends to increase at lower frequencies.

Due to the fact that the presented method is based on the room impulse response, it can also be applied to determine the steady-state and transient room responses. Therefore, it allows one to predict reverberation properties of rooms and their change after acoustic treatment. As the method is intended for the frequency range where the sound field exhibits modal behavior, it can be primarily used in the design and acoustic treatment of small rooms such as classrooms, performance studios, studio control rooms and lecture rooms, where the excitation of room modes may limit a correct perception of speech and music.

Acknowledgments

Additional information

The author declares no competing financial interests.

References

1. S. Maluski, B. Gibbs. The effect of construction material, contents and room geometry on the sound field in dwellings at low frequencies. Applied Acoustics, 65(1):31–44, 2004. DOI:10.1016/S0003-682X(03)00116-6

2. T. Welti, A. Devantier. Low-frequency optimization using multiple subwoofers. J. Audio Eng. Soc., 54(5):347–364, 2006.

3. M. Meissner, K. Wiśniewski. Influence of room modes on low-frequency transients: theoretical modeling and numerical predictions. J. Sound Vib., 448:19–33, 2019. DOI:10.1016/j.jsv.2019.02.012

4. M. Meissner, K. Wiśniewski. Investigation of damping effects on low-frequency steady-state acoustical behaviour of coupled spaces. R. Soc. Open Sci., 7(8):200514, 2020. DOI:10.1098/rsos.200514

5. M. Meissner. Application of modal expansion method for sound prediction in enclosed spaces subjected to boundary excitation. J. Sound Vib., 500:116041, 2021. DOI:10.1016/j.jsv.2021.116041

6. C. Papadopoulos. Redistribution of the low frequency acoustic modes of a room: a finite element-based optimisation method. Applied Acoustics, 62(11):1267–1285, 2001. DOI:10.1016/S0003-682X(01)00002-0

7. Z. Xiaotian, Z. Zhemin, C. Jianchun. Using optimized surface modifications to improve low frequency response in a room. Applied Acoustics, 65(9):841–860, 2004. DOI:10.1016/j.apacoust.2004.03.002

8. J. Rindel. Modal energy analysis of nearly rectangular rooms at low frequencies. Acta Acustica united with Acustica, 101(6):1211–1221, 2015. DOI:10.3813/AAA.918914

9. J. Rindel. Preferred dimension ratios of small rectangular rooms. JASA Express Letters, 1(2):021601, 2021. DOI:10.1121/10.0003450

10. J. Sarris. A new method for the determination of acoustically good room dimension ratios. AES 136th Convention, Berlin, Convention paper 9047, 2014.

11. M. Meissner. A novel method for determining optimum dimension ratios for small rectangular rooms. Archives of Acoustics, 43(2):217–225, 2018. DOI:10.24425/122369

12. H. Fuchs, X. Zha, H. Drotleff. Relevance and treatment of the low frequency domain for noise control and acoustic comfort in rooms. Acta Acustica united with Acustica, 91(5):920–928, 2005.

13. M. Meissner, T.G. Zieliński. Low-frequency prediction of steady-state room response for different configurations of designed absorbing materials on room walls. Proceedings of the 29th International Conference on Noise and Vibration Engineering (ISMA 2020) and the 8th International Conference on Uncertainty in Structural Dynamics (USD 2020), 463–477, 2020.

14. T. Vigran. Building acoustics. CRC Press, London, 2008.

15. S. Damelin, W. Miller Jr. The mathematics of signal processing. Cambridge University Press, New York, 2012.

16. L. Kinsler, A. Frey, A. Coppens, J. Sander. Fundamentals of acoustics. 4th edn, John Wiley & Sons, New York, 2000.

17. T. Cox, P. D'Antonio. Acoustic absorbers and diffusers: theory, design and application. 2nd edn, Taylor & Francis, New York, 2009.

18. T. Komatsu. Improvement of the Delany-Bazley and Miki models for fibrous sound-absorbing materials. Acoust. Sci. Technol., 29(2):121–129, 2008. DOI:10.1250/ast.29.121

19. A. Gray, J. Markel. A spectral-flatness measure for studying the autocorrelation method of linear prediction of speech analysis. IEEE Trans. Acoust. Speech Signal Process., 22(3):207–217, 1974. DOI:10.1109/TASSP.1974.1162572